Available online at www.sciencedirect.com
SCIENCE DIRECT
ELSEVIER
Earth and Planetary Science Letters 219 (2004) 93–110
EPSL
www.elsevier.com/locate/epsl

Isotopic evidence for Plio–Pleistocene environmental change at Gona, Ethiopia☆

Naomi E. Levin[a,*], Jay Quade[a], Scott W. Simpson[b], Sileshi Semaw[c], Michael Rogers[d]

[a] Department of Geosciences, University of Arizona, Tucson, AZ 85721, USA
[b] Department of Anatomy, Case Western Reserve University - School of Medicine, 10900 Euclid Avenue, Cleveland, OH 44106, USA
[c] CRAFT Institute, Indiana University, 419 N. Indiana, Bloomington, IN 47405, USA
[d] Department of Anthropology, Southern Connecticut State University, 501 Crescent Street, New Haven, CT 06515, USA

Received 3 May 2003; received in revised form 17 November 2003; accepted 10 December 2003

Abstract

A 4.5 Ma record of fluvial and lacustrine deposits is well exposed at Gona, in the Afar Depression of Ethiopia. We use isotopic values of pedogenic carbonate and fossil teeth to reconstruct Plio–Pleistocene environmental change at Gona. An increase in $\delta^{13}C$ values of pedogenic carbonates since 4.5 Ma points to a shift from woodlands to grassy woodlands in the early Pliocene, −10.4 to −3.9‰ (VPDB), to more open but still mixed environments in the late Pleistocene, −3.0 to −1.4‰ (VPDB). This pattern is also seen in isotopic records elsewhere in East Africa. However, at 1.5 Ma the higher proportion of C_4 grasses at Gona is largely a result of a local facies shift to more water-limited environments. The wide range of $\delta^{13}C$ values of pedogenic carbonate within single stratigraphic levels indicates a mosaic of vegetation for all time intervals at Gona that depends on depositional environment. Elements of this mosaic are reflected in $\delta^{13}C$ values of both modern plants and soil organic matter and Plio–Pleistocene soil carbonate, indicating higher amounts of C_4 grasses with greater distance from a river channel in both the modern and ancient Awash River systems. $\delta^{18}O$ values of pedogenic carbonates increase up-section from −11.9‰ in the early Pliocene to −6.4‰ (VPDB) in the late Pleistocene. The wide range of $\delta^{18}O$ values in paleovertisol carbonates from all stratigraphic levels probably reflects short-term climate changes and periods of strong evaporation throughout the record. Based on the comparison between $\delta^{18}O$ values of Plio–Pleistocene pedogenic carbonates and modern waters, we estimate that there has been a 6.5‰ increase in mean annual $\delta^{18}O$ values of meteoric water since 4.5 Ma. $\delta^{18}O$ values of pedogenic carbonate from other East African records indicate a similar shift. Increasing aridity and fluctuations in the timing and source of rainfall are likely responsible for the changes in $\delta^{18}O$ values of East African pedogenic carbonates through the Plio–Pleistocene.

* Corresponding author. Present address: Department of Geology and Geophysics, University of Utah, 135 S. 1460 East, Salt Lake City, UT 84112-0111, USA. Tel.: +1-801-403-9070; Fax: +1-801-581-7065.
E-mail address: nlevin@mines.utah.edu (N.E. Levin).

☆ Supplementary data associated with this article can be found at doi:10.1016/S0012821X03007076

0012-821X/04/$ – see front matter © 2004 Elsevier B.V. All rights reserved.
doi:10.1016/S0012-821X(03)00707-6

Keywords: Ethiopia; East Africa; paleoclimate; isotopes; Plio–Pleistocene; paleosols

1. Introduction

Sediments at Gona, in the Afar region of Ethiopia, contain a rich record of Plio–Pleistocene fossils and stone tools [1–3] (Figs. 1 and 2). There is great interest in placing this and other East African fossil and archeological records within the context of environmental change. Many climate studies suggest an increase in aridity and climate variability in Plio–Pleistocene East Africa, based on evidence of heightened dust fluxes, increased coastal upwelling, faunal change and grassland expansion [4–7]. Of particular relevance to human evolution is the expansion of East African grasslands, as recorded by carbon isotopes from pedogenic carbonate and fossil teeth. Some records from East African sites also display higher oxygen isotopic values of pedogenic carbonates in the late Pleistocene, although the paleoenvironmental significance of this remains unclear [8,9].

Stable isotopic studies have just begun in the Awash Basin, in contrast to well-documented isotopic records from elsewhere in East Africa [10–12]. Previous studies of the Plio–Pleistocene paleoenvironments of Hadar (northeast of the Gona study area) (Fig. 1) primarily rely on faunal, palynologic and sedimentologic evidence, and attribute much of the environmental change to dramatic decreases in basin elevation [13–15]. The rich geologic archive at Gona provides an excellent opportunity to distinguish local environmental phenomena from regional climate changes, and to place the human evolutionary record from 4.5 to 0.6 Ma in a firm paleoenvironmental context. This paper uses isotopic values of pedogenic carbonate and fossil teeth to reconstruct paleoenvironmental change over this critical time span for human evolution.

2. Background

2.1. Geology and geochronology

The Gona project area is bounded to the east by the Awash River, a large river system that drains the western escarpment of the Afar Depression (Fig. 1). The Kada Gona drainage divide and the Busidima/Asbole drainage bound the Gona project area to the northeast and south, respectively. The As Duma Fault, a basin-bounding, north-trending normal fault, bisects the project area, dividing the older Sagantole Formation to the west from younger basin-fill deposits to the east [16]. The Sagantole Formation is composed of lacustrine claystones, travertines, carbonate-rich vertic paleosols, and volcaniclastic sediments. The sediments of the Sagantole Formation are intercalated with basalts and tuffs and cut by dikes and multiple normal faults. An air-fall tuff, dated by $^{40}Ar/^{39}Ar$ analyses from single plagioclase crystals, establishes 4.56 Ma as the maximum age for the base of the Sagantole Formation at Gona (J. Quade, unpublished data) (Fig. 2). The paleosols and fossil teeth sampled for isotopic analysis in this study lie 10–20 m above this tuff and probably represent a time interval < 100 kyr. This error estimate and those listed in the following descriptions of the Gona sediments are approximations based on uniform sedimentation rates between tuff deposits dated by $^{40}Ar/^{39}Ar$ analyses.

Basin fill east of the As Duma Fault consists of the Hadar and Busidima formations. The Hadar Formation contains fluvial and lacustrine sediments deposited in the central axis of the basin between $\sim$3.4 and 2.9 Ma (Fig. 2). The geochronology of the Hadar Formation is well established and based largely upon $^{40}Ar/^{39}Ar$ dates from major and minor tuffs exposed in the Hadar project area north and east of the Kada Gona drainage divide [17]. Some of these tuffs, including the well-known SHT, Triple Tuffs and KHT, as well as key marker sands and lacustrine beds, extend into the Gona project area. We used these dated horizons to estimate the ages of carbonate samples, assuming uniform sedimentation rates. The error of our age estimates is < 100 kyr.

A major disconformity (2.9–2.7 Ma), closely bounded by two dated tuffs, separates the Busidi-

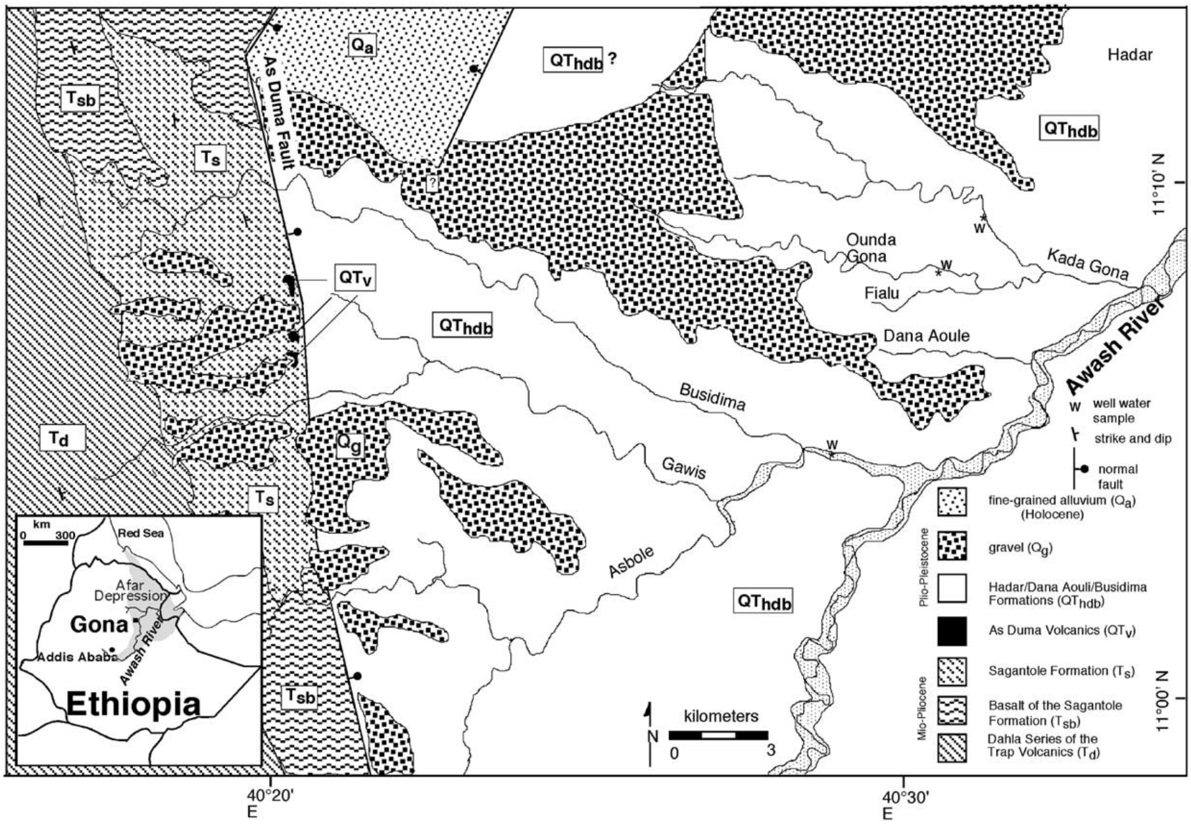

Fig. 1. Geologic map of Gona, Afar, Ethiopia.

ma Formation from the Hadar Formation below (Fig. 2) [16]. This disconformity marks a change in depositional style from a mix of fluvial and lacustrine deposition in the Hadar Formation to solely fluvial deposition in the Busidima Formation. The lower Busidima Formation is characterized by multiple fining-upward sequences deposited by a coarse-grained, meandering river system that flowed northeastward along the axis of the paleo-Awash valley [16]. In contrast, the upper Busidima Formation consists of paleosols and minor channel deposits associated with tributary river systems on distal alluvial fans. We use the presence of the Boolihinan Tuff ($\sim$1.5 Ma) to date the major facies shift that separates the lower and upper Busidima Formation [16]. Age assignments for pedogenic carbonate samples from the Busidima Formation are conservatively $<$200 kyr but likely $<$100 kyr.

Tephrostratigraphic correlations indicate that the top of the Busidima Formation is $\sim$0.6 Ma [16]. Therefore, pedogenic carbonates formed on the alluvial fan gravels that cap the Busidima Formation likely date from 0.6 to 0 Ma.

2.2. C_3/C_4 plant distribution and carbon isotopes

Carbon isotopic values ($\delta^{13}C$) of soil organic matter and pedogenic carbonate can be used to reconstruct the proportion of trees and grasses present during soil formation. C_3 and C_4 plants fractionate carbon isotopes through different metabolic pathways. The C_3 pathway discriminates more strongly against ^{13}C than the C_4 pathway and produces plant matter with lower $\delta^{13}C$ values. In East Africa, the $\delta^{13}C$ values of C_3 and C_4 plants range from -31.4 to -24.6‰ and -14.1 to -11.5‰, respectively [18]. The range in values

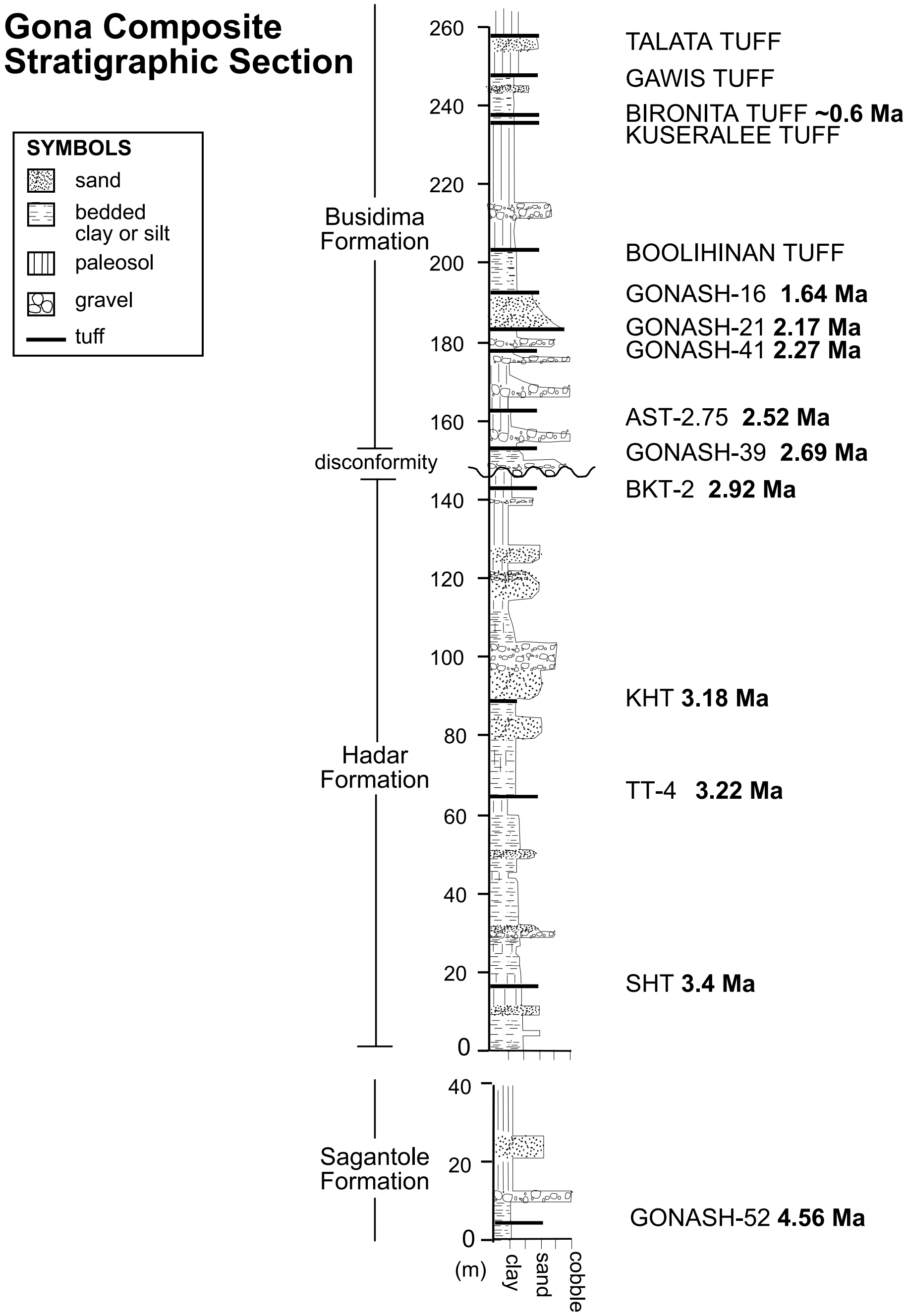

Fig. 2. Composite stratigraphic section of the Sagantole, Hadar and Busidima Formation exposed in the Gona project area. Ages listed next to tuffs are either from $^{40}Ar/^{39}Ar$ dates or from tephrostratigraphic correlation [16,17].

within C_3 and C_4 plants primarily depends on water availability, and also canopy cover for C_3 plants. Globally, C_4 grasses dominate warm growing season ecosystems, and in East Africa most low altitude grasses (< 2500 m) are C_4 [19]. Any C_3 grasses that do grow at low altitudes in East Africa grow in damp habitats as understory grasses in forests [20].

The proportion of C_3 to C_4 vegetation on a landscape is recorded by carbon isotopic values of the underlying leaf litter, soil organic matter, and soil carbonates formed from plant-respired soil CO_2 [21]. $\delta^{13}C$ values of pedogenic carbonate ($\delta^{13}C_{PC}$) reflect $\delta^{13}C$ values of soil CO_2, which is determined by the isotopic composition of overlying vegetation at moderate to high soil respiration rates. At soil depths greater than 30 cm, $\delta^{13}C_{PC}$ values differ from $\delta^{13}C$ values of the overlying vegetation by +13.5–16.6‰ [22].

$\delta^{13}C$ values of fossil tooth enamel ($\delta^{13}C_{enamel}$) record the proportion of C_3 to C_4 plants consumed by an animal during enamel formation early in life as teeth develop [23]. Although past studies have provided a range of enrichment factors between $\delta^{13}C_{enamel}$ and dietary $\delta^{13}C$ values, recent work shows that carbon isotope ratios in herbivore teeth are enriched in ^{13}C by 14.1‰ relative to the plant matter consumed [24].

The isotopic composition of atmospheric CO_2 varies with fluxes in the global carbon cycle [25]. Any variation in the $\delta^{13}C$ value of atmospheric CO_2 alters $\delta^{13}C$ values of vegetation and thus changes the meaning of $\delta^{13}C$ values for both pedogenic carbonate and tooth enamel. However, we do not account for the effect of such changes in this study because the small changes in atmospheric $\delta^{13}C$ values between the Pliocene and today would not alter our large-scale interpretations of relative C_3 and C_4 abundance from $\delta^{13}C$ values of pedogenic carbonates and fossil tooth enamel [26].

2.3. Oxygen isotopes in meteoric waters and soil carbonate

$\delta^{18}O$ values of meteoric water ($\delta^{18}O_{MW}$) reflect air temperature and the amount, source and seasonal distribution of rainfall [27]. $\delta^{18}O_{MW}$ values typically increase with increased air temperature and decrease with higher rainfall amounts and increased altitude [27]. Modern $\delta^{18}O_{MW}$ values recorded in East Africa vary seasonally as rainfall amount and moisture sources change [28].

$\delta^{18}O$ values of pedogenic carbonate ($\delta^{18}O_{PC}$) depend on soil temperature and the $\delta^{18}O$ values of soil water ($\delta^{18}O_{SW}$) during carbonate formation [21,29]. At depths greater than 30 cm, soil temperatures approach mean annual ambient temperatures [30]. $\delta^{18}O_{PC}$ values also vary with soil depth. Quade et al. [29] attribute the decrease in $\delta^{18}O_{PC}$ values with depth in the soil either to greater evaporative enrichment near the soil surface or to preferential infiltration of isotopically depleted rainfall. In the absence of soil water evaporation, $\delta^{18}O_{SW}$ should be roughly equivalent to $\delta^{18}O_{MW}$ values. If we assume that carbonate always forms in the presence of soil moisture that is solely determined by $\delta^{18}O_{MW}$ and temperature, we then can use $\delta^{18}O_{PC}$ values to estimate mean annual $\delta^{18}O_{MW}$ values. However, hot and arid environments, like those in East Africa, increase the likelihood of soil water evaporation and produce $\delta^{18}O_{SW}$ values that are higher than mean annual $\delta^{18}O_{MW}$ values. Consequently, assuming constant temperatures of formation, any estimates of mean annual $\delta^{18}O_{MW}$ values from $\delta^{18}O_{PC}$ values are maxima.

2.4. Carbonate formation

Secondary carbonates at Gona include both pedogenic and non-pedogenic (groundwater and spring) forms. The distinction between the two types of carbonates is critical in isotopic studies because the relationship between $\delta^{13}C_{PC}$ values and vegetation cover is only established for soils. Pedogenic carbonates are abundant in the vertic paleosols at Gona. To qualify as pedogenic, carbonate must be found within a zone of carbonate formation (Bk horizon) and it must be associated with other pedogenic features. At Gona, pedogenic carbonates are associated with vertic features like the development of ped structure, clay cutans or slickensides on ped faces. The development of these features varies with the degree of soil formation as determined by both environmental conditions and time. Within a soil horizon, carbonate can be dispersed throughout the matrix or can take the form of stringers, nodules, rhizoliths, clast coatings or platey vertic fracture fill.

Non-pedogenic carbonates at Gona are formed by ground or spring waters and can take the form of nodules, rhizoliths, ledges, travertines, and sparry precipitate in the interstices of gravels. They are distinguished from pedogenic carbonates because they are not associated with a soil horizon or other pedogenic features.

3. Methods

Pedogenic carbonates were sampled at least 30 cm below the upper paleosol contact to ensure that $\delta^{13}C_{PC}$ values represent the $\delta^{13}C$ values of soil CO_2 (and hence the fraction of C_3/C_4 biomass) and to reduce the potential influence of soil water evaporation on $\delta^{18}O_{PC}$ values. The upper paleosol contact is usually a conservative estimate of a former land surface because erosion can remove part of the upper soil horizons. Most upper paleosol contacts were recognized by a major change in lithology, such as the scour of a fluvial gravel.

Pedogenic carbonate nodules were first broken to reveal their internal structure and to avoid analysis of any non-pedogenic spar found in vugs and small veinlets. Fifty-three nodules (206 analyses) were microsampled to investigate the isotopic variation between micrite and spar within single nodules and to characterize the variation within the micritic portions. Microsampling was performed under a binocular microscope with a 0.5 mm drill bit at 2 mm intervals along an interior cross-section. All carbonate samples were heated at 400°C for 3 h in vacuo and processed using an automated sample preparation device (Kiel III) attached directly to a Finnigan MAT 252 mass spectrometer at the University of Arizona. $\delta^{18}O$ and $\delta^{13}C$ values were normalized to NBS-19 based on internal lab standards. Precision of repeated standards is ± 0.1‰ for $\delta^{18}O$ and ± 0.06‰ for $\delta^{13}C$ (1σ).

Fossil tooth enamel was prepared for analysis of the $\delta^{13}C$ value its structural carbonate following a procedure adapted from O'Neil et al. [31]. Enamel was removed from the dentine with a 0.5 mm drill bit. Enamel powder was pretreated with 2% H_2O_2 and reacted in an ultrasonic bath to remove remnant organic matter. Samples were then reacted with 1 M acetic acid for 30 minutes in an ultrasonic bath, rinsed with distilled water, dried at 80°C and reground. Enamel was reacted with 3 ml 100% H_3PO_4 at 50°C, and the resultant CO_2 was purified cryogenically. Carbon isotopes of the purified gas were measured on a Finnigan Delta S mass spectrometer.

Plant matter and bulk soil organic matter were collected on the floodplain of the modern Awash River. Plant matter was ground and soil organic matter was sieved through a 250 μm mesh sieve, pretreated with 2 M HCl and rinsed with deionized water. Organic $\delta^{13}C$ values were measured using an automated CHN analyzer (Costech) connected to a Finnigan Delta-plus XL continuous-flow mass spectrometer. Internal lab standards are calibrated relative to NBS-22 and USGS-24. Precision of repeated internal standards is ± 0.09‰ for $\delta^{13}C$ (1σ).

Stable isotope composition of water was measured on a Finnigan MAT Delta-S gas ratio mass spectrometer using two automated sample preparation devices. $\delta^{18}O$ values were measured using CO_2 equilibration at 15°C for a minimum of 8 h [32]. δD values were measured by reducing the water on chromium at 750°C and direct transfer of H_2 into the mass spectrometer [33]. Samples were normalized to VSMOW and VSLAP based on secondary standards. Repeated standards have a standard deviation of 0.06‰ for $\delta^{18}O$ values and 0.8‰ for δD values.

Carbonate, teeth and organic matter isotopic results are reported using standard δ‰ notation relative to VPDB, whereas $\delta^{18}O$ values of waters are presented relative to VSMOW.

4. Pedogenic vs. non-pedogenic carbonates

4.1. Carbonate morphologies and textures

Pedogenic carbonate nodules range from 2 to 30 mm in diameter and reflect stage II and stage

III carbonate development for non-clastic parent materials [34]. Petrographic examination showed that nodule texture is dominantly micritic, although distinct concentrations of spar are common. Spar and microspar crystals concentrate in vugs and veins, and sometimes surround detrital lithic grains, quartz and clay. Dendritic manganese often accompanies the spar. Both rhizoliths and vertic fracture fill are dominantly micritic but often contain spar-filled veins and vugs, and dendritic manganese threads.

Non-pedogenic carbonates from the Gona deposits were also studied in thin section and sampled for isotopic analysis. Sparry calcite cements many of the large fluvial cobble conglomerates in the lower Busidima Formation. In addition, micritic travertine and very coarse, euhedral calcite crystals are present in the Sagantole Formation. The euhedral calcite is found in thick (> 2 cm) veins and in the hollow cavities of fossil bone. Travertines often contain freshwater snails and bivalves.

4.2. *Isotopic results from carbonate morphologies and textures*

$\delta^{18}O$ values (-6.0 ± 0.5‰, 1σ, $n = 5$) of the sparry cements from the conglomerates in the lower Busidima Formation lie within the same range as values for spar and micrite in pedogenic nodules (Tables 1 and 2[1]). $\delta^{13}C$ values of conglomerate spar average -4.5 ± 0.1‰ (1σ; $n = 5$). $\delta^{13}C$ and $\delta^{18}O$ values of coarse euhedral calcite from the Sagantole Formation average -6.3 ± 1.1‰ and -16.5 ± 4.5‰ (1σ; $n = 5$). Micritic travertines from the Sagantole Formation average -6.9 ± 0.7‰ and -11.4 ± 0.7‰ (1σ; $n = 3$) for $\delta^{13}C$ and $\delta^{18}O$ values respectively.

$\delta^{13}C$ and $\delta^{18}O$ values of rhizolith and vertic fracture fill fall within the same range of values as nodular carbonate sampled throughout the section (Figs. 3a and 5a).

[1] See online version of this article.

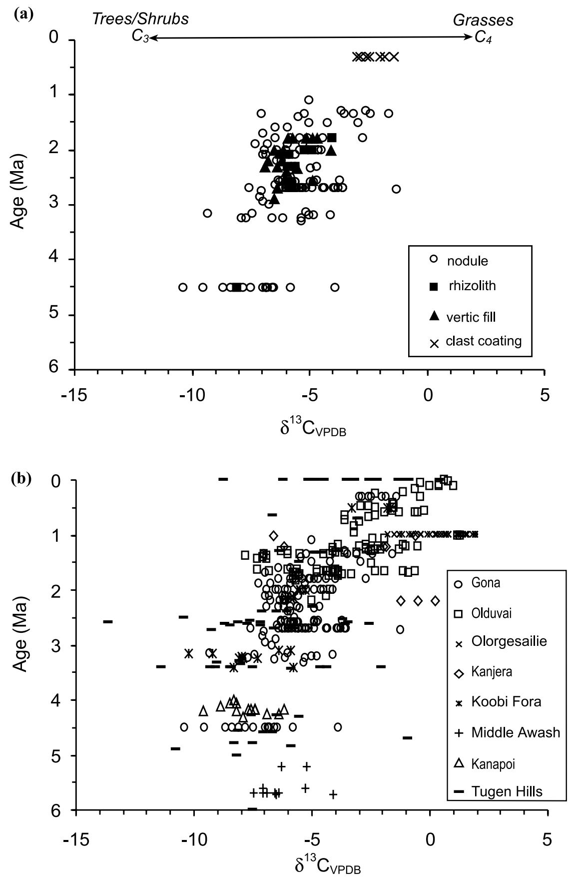

Fig. 3. $\delta^{13}C_{PC}$ values from (a) Gona and (b) East Africa sites: Olduvai [9,40], Olorgesailie [41], Kanjera [43], Koobi Fora [8], Middle Awash [10], Kanapoi [42] and Tugen Hills [46].

4.3. *Carbonate formation and diagenetic alteration*

Spar-filled vugs and veins are uncommon in modern soil carbonate but are often found in otherwise unaltered fossil pedogenic carbonates [35,36]. High $\delta^{18}O$ values of spar within nodules of all ages at Gona indicate that the spar formed at low temperatures and was not subjected to hydrothermal alteration. However, we exclude the isotopic results of the nodule spar from the data used in our paleoenvironmental reconstruction because its mode of formation is unclear.

The presence of coarse, euhedral calcite crystals in veins and volcanic dikes cutting the Sagantole Formation points to hydrothermal activity in the older deposits. Some of the euhedral calcite yields very low $\delta^{18}O$ values, as low as −23.4‰, and clearly formed at elevated temperatures. The highest $\delta^{18}O$ value (−12.8‰) from euhedral calcite is close to the lowest $\delta^{18}O_{PC}$ value (−11.9‰) from the Sagantole Formation, and might have either a moderately hydrothermal or a low temperature origin. However, micritic travertines from the Sagantole Formation, which show no textural evidence of diagenetic alteration, have a minimum $\delta^{18}O$ value (−12.1‰) close to the minimum $\delta^{18}O_{PC}$ value (−11.9‰) (Table 2[1]). The presence of intact primary textures in both the pedogenic carbonate and the travertine suggests that their low $\delta^{18}O$ values reflect the primary conditions of carbonate formation. In addition to the textural, isotopic and morphologic evidence, the abundance of reworked carbonate nodules in minor channel deposits of all the formations sampled suggests that these carbonates are pedogenic and not diagenetic.

Fossil teeth analyzed for this study are well preserved, with little visible evidence (discoloration, physical breakdown) of alteration. In general, $\delta^{13}C$ values of fossil enamel are highly resistant to diagenesis [37].

5. $\delta^{13}C$ values of pedogenic carbonate and fossil teeth

5.1. Sagantole Formation

$\delta^{13}C_{PC}$ values from the Sagantole Formation (4.5 Ma) average −7.4‰ ± 1.6 (1σ; $n = 15$) and range from −10.4 to −3.9‰ (Fig. 3a). The range of values indicates that C_4 grass cover in the Gona area was approximately 10–60% at ∼4.5 Ma.

$\delta^{13}C_{enamel}$ values of Hippopotamidae ($n = 6$), Proboscidea ($n = 1$), Bovidae ($n = 3$), and Suidae (all *Nyanzachoerus jaegeri*) ($n = 6$) from the Sagantole Formation range from −14.1 to +0.1‰ ($n = 16$) (Table 3[1]). All of the $\delta^{13}C$ values of tooth enamel, except two Hippopotamidae samples and the Proboscidea sample, are evidence of C_4-dominated diets. At 4.5 Ma there must have been enough C_4 grass on the landscape to support animals with grazing (C_4) adaptations.

5.2. Hadar and Busidima formations

$\delta^{13}C_{PC}$ values from the Hadar Formation (3.3–2.9 Ma) average -6.6 ± 1.4‰ (1σ; $n = 17$) (Fig. 3a). Average $\delta^{13}C_{PC}$ values increase from -5.5 ± 1.1‰ (1σ; $n = 97$) in the lower Busidima Formation (2.9–1.5 Ma) to -4.0 ± 1.5‰ (1σ; $n = 13$) in the upper Busidima Formation (∼1.5–0.5 Ma). $\delta^{13}C$ values from carbonate clast coatings on the middle Pleistocene gravels average -2.3 ± 0.6‰ (1σ; $n = 7$).

$\delta^{13}C_{PC}$ values indicate a steady increase in C_4 grass cover, from approximately 20–55% in the Hadar Formation to 35–75% in the upper Busidima Formation. In the Hadar and lower Busidima formations, axial, rift-system lakes and rivers hosted water-dependent trees, shrubs and edaphic grasses (grasses rooted in a shallow floodplain water table) [16]. Due to the continuous presence of an axial depositional system, the increase in grasses during this time period must reflect environmental change independent of depositional environment. However, at ∼1.5 Ma the axial river environments of the lower Busidima Formation were replaced by more marginal environments characterized by deeper water tables, dry alluvial fans, and seasonally active tributaries of the paleo-Awash. Consequently, we view the increase in C_4 grasses in the upper Busidima Formation as the result of a local facies shift.

5.3. C_3/C_4 plant distribution on the floodplain of the modern Awash River

We measured the variation in $\delta^{13}C$ values of vegetation and soils on the modern Awash floodplain and used the results as a comparative model for the variation in $\delta^{13}C_{PC}$ values from the lower Busidima Formation. Based on sedimentologic similarities, the modern Awash River is an appropriate modern analog for the depositional setting of the lower Busidima Formation [16]. Near Gona, the Awash River is an entrenched meandering system flanked by an approximately 300 m wide swath of thick riparian woodland that is bordered by edaphic grasslands. The $\delta^{13}C$ values of both soil organic matter and plant matter increase with distance from the Awash channel (Fig.

4a; Table 4[1]). Plant $\delta^{13}C$ values from within the dense riparian woodland average -27.9 ± 1.5‰ (1σ; $n = 9$) and those of edaphic grasses average -15.0 ± 3.3‰ (1σ; $n = 3$). Within the C_3-rich riparian woodland, soil organic matter averages -23.7 ± 1.4‰ (1σ; $n = 9$) and is enriched in ^{13}C relative to the vegetation directly overlying it. Higher soil organic matter $\delta^{13}C$ values in the riparian woodland might be due to ^{13}C-enriched microbial and fungal residues in the soil, incorporation of plant litter with pre-industrial $\delta^{13}C$ values when atmospheric $\delta^{13}C$ values were ~ 1.3‰ higher (Seuss effect), or a shift in the distribution of C_3 and C_4 plants [38]. In the open floodplain dominated by edaphic grassland, $\delta^{13}C$ values of soil organic matter average -20.1 ± 2.9‰. The

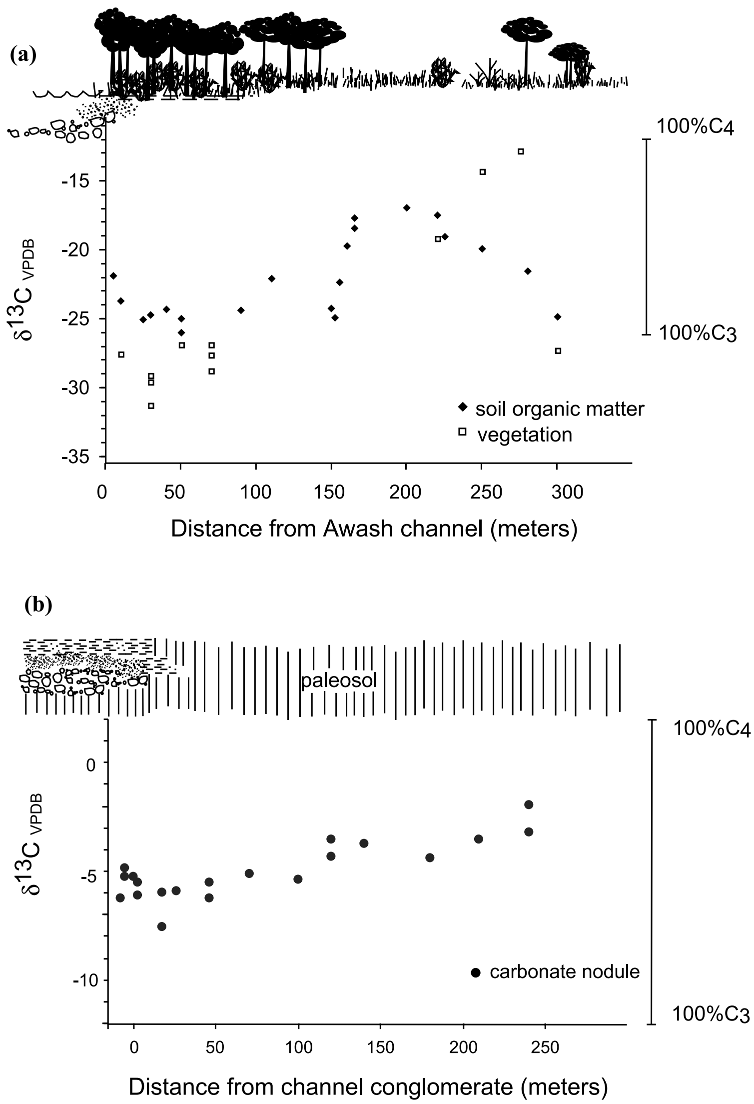

Fig. 4. Lateral transect results. (a) $\delta^{13}C$ values of modern vegetation and soil organic matter and distance from the Awash River channel. (b) $\delta^{13}C_{PC}$ values in a paleosol lateral to lower Busidima Formation conglomerate. The drawing overlying each plot represents the sampling context of each transect.

more negative values in the grassland sediment can be specifically related to the local presence of trees.

We use the isotopic relationships on the modern floodplain to clarify the paleoecologic context of paleo-Awash floodplain deposits in the lower Busidima Formation. For this comparison, we selected a ∼2.7 Ma paleosol exposure that is lateral to a conglomerate, representing a paleo-channel at the limit of its lateral migration and its associated floodplain. We sampled the paleosol for soil carbonates at 25 m intervals for approximately 250 m lateral to the conglomerate–paleosol transition. The $\delta^{13}C_{PC}$ values increase from −7.6 to −2.0‰ with increasing lateral distance from the conglomerate–paleosol transition (Fig. 4b). The increase in $\delta^{13}C_{PC}$ values records the transition from riparian woodland to grassland, in strong correspondence to the modern analog.

However, one difference between the modern analog and fossil results is that we obtain no $\delta^{13}C_{PC}$ values that represent end-member C_3 or C_4 conditions in the lower Busidima Formation as we do in the modern Awash floodplain. There are at least three ways to interpret this difference: (1) there were never any pure C_3 or C_4 vegetation stands lateral to the channel; (2) $\delta^{13}C_{PC}$ values represent a time-average of fluctuating vegetation zones, with the rapid migration of a river channel and its associated riparian woodland an end-member C_3 value will not be recorded; or (3) soil CO_2 mixes laterally, reducing the isotopic contrast between adjacent stands of pure C_3 and C_4 vegetation.

Explanation (1) is unlikely because higher $\delta^{13}C_{PC}$ values in the Pliocene indicate a greater overall presence of C_3 vegetation than in the modern environment. A nearly pure C_3 gallery forest borders the modern Awash River. If the modern Awash River is an appropriate analog for the paleo-Awash system we should expect a greater or equal amount of C_3 vegetation adjacent to a major river channel in the Pliocene.

In our view, explanation (2) is the most plausible. If C_3 vegetation is restricted to river banks, the end-member C_3 signal would not be recorded in $\delta^{13}C_{PC}$ values because the period of carbonate formation (10^3–10^4 years) exceeds the typical residence time of vegetation and channel position (10–10^2 years). Pedogenic carbonate forming beneath a C_3 riparian woodland will either be eroded by the river's cut bank or become increasingly distal to the C_3-rich riparian vegetation belt as the river channel migrates.

Explanation (3), lateral soil CO_2 mixing, is untested and requires measurements of $\delta^{13}C$ values of modern soil CO_2 across riparian woodland and edaphic grassland vegetation zones.

5.4. Regional grassland expansion

The increase in $\delta^{13}C_{PC}$ values evident in other East African paleosol records points to an expansion of C_4 grasses throughout the Plio–Pleistocene (Fig. 3b). Although there is evidence of C_4 vegetation as early as 15.3 Ma in East Africa, C_4 grasses became a substantial part of herbivore diets by the latest Miocene and came to dominate most East African landscapes after 1.7 Ma [6,39].

$\delta^{13}C$ values of 4.5 Ma tooth enamel and pedogenic carbonate demonstrate the significant presence of grasses by the early Pliocene at Gona. Slightly older environments (5.54–5.77 Ma), south of Gona in the Middle Awash Sagantole Formation, have been interpreted as closed and wet woodlands from fauna [10]. However, $\delta^{13}C_{PC}$ values from the Middle Awash also indicate the presence of considerable C_4 grass mixed with woodlands. The range of $\delta^{13}C_{PC}$ values from the Middle Awash, −7.5 to −4.1‰ ($n = 11$) [10] is similar to the range of $\delta^{13}C_{PC}$ values, −10.4 to −3.9‰ ($n = 15$) from the Sagantole Formation at Gona.

$\delta^{13}C_{PC}$ values from the Hadar and lower Busidima formations parallel those of other East African soil carbonates of the same age. $\delta^{13}C_{PC}$ values from Koobi Fora and Olduvai show similar increases in C_4 vegetation, as do values from the shorter records at Olorgesailie, the Middle Awash, and Kanapoi (Fig. 3b) [8–10,40–43]. As at Gona, the wide range in $\delta^{13}C_{PC}$ values from every study area at any given time interval indicates considerable heterogeneity in the distribution of C_3 and C_4 vegetation.

6. δ^{18}O values of pedogenic carbonates and modern waters

6.1. δ^{18}O values Plio–Pleistocene carbonates

Two features of the Gona $\delta^{18}O_{PC}$ record have significant implications for both local environmental variability and regional climate change. The first feature is the considerable scatter in $\delta^{18}O_{PC}$ values (typically > 5‰) at every stratigraphic interval (Fig. 5a). The second feature is the up-section increase in both mean and minimum $\delta^{18}O_{PC}$ values. Mean $\delta^{18}O_{PC}$ values increase from −7.8‰ in 4.5 Ma to −4.5‰ < 0.6 Ma. Minimum $\delta^{18}O_{PC}$ values increase from −11.9‰ in 4.5 Ma to −6.4‰ < 0.6 Ma.

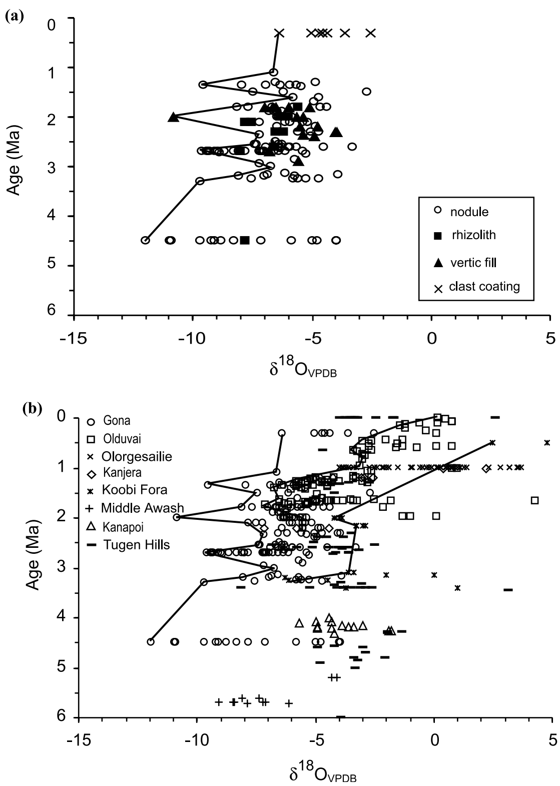

Fig. 5. $\delta^{18}O_{PC}$ values from (a) Gona, with a line connecting minimum values for each 100 kyr time interval, and (b) East African sites: Olduvai [9,40], Olorgesailie [41], Kanjera [43], Koobi Fora [8], Middle Awash [10], Kanapoi [42] and Tugen Hills [46]. Lines connect the minimum values for the Gona, Koobi Fora and Olduvai records.

These patterns in the $\delta^{18}O_{PC}$ record can be explained in terms of the three main determinants of $\delta^{18}O_{PC}$ values: mean annual $\delta^{18}O_{MW}$ values, soil temperature and soil water evaporation. $\delta^{18}O_{MW}$ values and soil temperature are related to $\delta^{18}O_{PC}$ values according to the following expression: $1000 \ln\alpha_{calcite-water} = 18.03\times(10^3\ T^{-1})-32.42$, where α is the fractionation factor, T is the temperature in Kelvin and $\alpha_{calcite-water} = (\delta^{18}O_{PC}+1000)/(\delta^{18}O_{SW}+1000)$ [44]. At constant $\delta^{18}O_{MW}$ values, large changes in soil temperature result in only small changes in $\delta^{18}O_{PC}$ values. By comparison, evaporative enrichment of ^{18}O in soil water can produce large increases in associated $\delta^{18}O_{PC}$. As such, we interpret the broad scatter of $\delta^{18}O_{PC}$ values at any one stratigraphic level at Gona as likely produced by: (1) the intense but variable evaporation of soil water prior to carbonate precipitation and (2) short-term fluctuations in mean annual $\delta^{18}O_{MW}$ values associated with shifting climatic conditions within the stratigraphic resolution at Gona (~100 kyr). The change in soil temperature required to produce a 5‰ range in $\delta^{18}O_{PC}$ values within 100 kyr is unrealistically high ($\Delta T_{soil} = 25$°C).

The up-section increase in mean and minimum $\delta^{18}O_{PC}$ values through the Plio–Pleistocene is not unique to Gona and is also evident in other East African deposits, as we will discuss later. A combination of higher mean annual $\delta^{18}O_{MW}$ values and increasing soil water evaporation is likely responsible for the long-term increase in $\delta^{18}O_{PC}$ values. In the absence of additional data the relative contributions of changing $\delta^{18}O_{MW}$ values and evaporative conditions are difficult to determine. For the Gona data set, however, we do have an additional constraint. We can use modern $\delta^{18}O_{MW}$ values to show that mean annual $\delta^{18}O_{MW}$ values must have increased significantly between the early Pliocene and the Present, although the exact timing of this shift is not clear.

6.2. $\delta^{18}O_{MW}$ values

To explore the relative effect of changing $\delta^{18}O_{MW}$ values and soil water evaporative conditions on $\delta^{18}O_{PC}$ values we consider the lowest (and therefore least evaporated) $\delta^{18}O_{PC}$ value (−11.9‰) from the base of the Gona record (Fig. 5a). We reconstruct a $\delta^{18}O_{MW}$ value of −9.4‰ for this carbonate sample at 4.5 Ma by assuming a soil temperature equivalent to the approximate mean annual temperature at Gona today, 26°C. This is a maximum $\delta^{18}O_{MW}$ estimate because the soil water, which originated as meteoric water, likely experienced at least some evaporation before carbonate formation. If soil water evaporation were the sole determinant of increasing $\delta^{18}O_{PC}$ values, we could generate the rest of the Gona $\delta^{18}O_{PC}$ record by holding the calculated early Pliocene $\delta^{18}O_{MW}$ value constant at −9.4‰ and increasing soil water evaporation.

Our measurements of modern groundwaters and river waters help to constrain modern $\delta^{18}O_{MW}$ values at Gona. Groundwater samples were obtained from open wells in dry tributaries to the Awash River at Gona in the dry season, February 1999–2001 (Fig. 1; Table 5[1]) and yielded a range of $\delta^{18}O$ values ($\delta^{18}O_{GW}$) from −0.8 to 1.1‰ and δD values of 0.05 to 11.01‰ (VSMOW). $\delta^{18}O$ and δD values of river waters, sampled from high to low elevations, yielded a range of −0.03 to +2.4‰ and +7.1 to +16.4‰ (VSMOW), respectively (Table 5[1]). Values from a small spring (Entoto) in the Awash headwaters near Addis Ababa gave $\delta^{18}O$ and δD values of −2.6 and −7.3‰ (VSMOW), respectively. Most isotopic results from both surface water and the Gona groundwater plot to the right of the global meteoric water line (GMWL) and the Addis Ababa meteoric water line (AMWL), indicating varying degrees of evaporative enrichment (Fig. 6).

To estimate modern mean annual $\delta^{18}O_{MW}$ values at Gona we reconstruct the initial isotopic values of these waters, prior to evaporation, by connecting these points back to the GMWL along evaporative enrichment lines, whose slope varies from 4.5 to 3.9 based on 50% or 0% humidity [45]. Using the evaporative enrichment lines, the unevaporated $\delta^{18}O_{MW}$ values range from −2.9‰ to −0.8‰ (Fig. 6). We compare the Gona $\delta^{18}O_{GW}$ and δD_{GW} values to the GMWL because it closely represents the waters from most stations

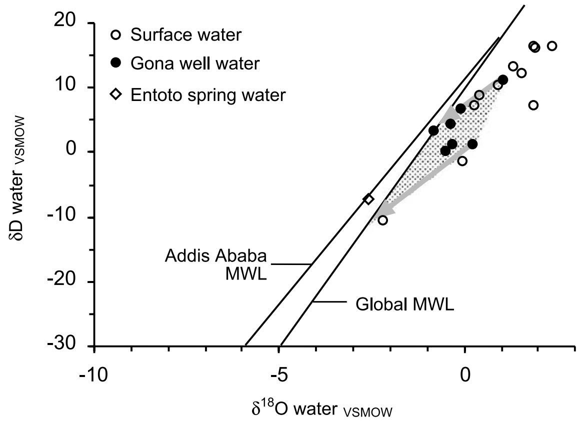

Fig. 6. δD and $\delta^{18}O$ values of waters plotted with the Addis Ababa ($\delta D = 6.95\delta^{18}O + 11.51$) and global ($\delta D = 8\delta^{18}O + 10$) meteoric water lines [28]. Reconstructed minimum and maximum unevaporated $\delta^{18}O_{MW}$ values, −2.9‰ and −0.78‰ (VSMOW), respectively, are calculated from Gona well waters. The degree of evaporative enrichment in ^{18}O of Gona well water with respect to meteoric water is determined from the intersection of the GMWL and the evaporative lines. Evaporative lines (marked by gray arrows) with slopes of 3.9 (0% humidity) and 4.5 (50% humidity) are used to reconstruct $\delta^{18}O_{MW}$ values.

in East Africa [28]. We do not use the AMWL because high elevation (2360 m), heavy rainfall (1219 mm/yr) and high mean annual $\delta^{18}O_{MW}$ value (−1.31% VSMOW) make rainfall in Addis Ababa isotopically anomalous [28].

If valid, these modern $\delta^{18}O_{MW}$ values show that increased soil water evaporation is not the sole determinant of increasing $\delta^{18}O_{PC}$ values at Gona. The comparison between the modern $\delta^{18}O_{MW}$ value, −2.9‰, and the calculated 4.5 Ma $\delta^{18}O_{MW}$ value, −9.4‰, shows that $\delta^{18}O_{MW}$ values must have increased by at least 6.5‰ between the early Pliocene and the Present (Fig. 7). This conclusion does not exclude the role of evaporation in influencing $\delta^{18}O_{PC}$ values at Gona. It merely demonstrates the minimum shift in $\delta^{18}O_{MW}$ values required to produce the observed differences between estimated modern $\delta^{18}O_{MW}$ values and Pliocene $\delta^{18}O_{PC}$ values.

6.3. Regional $\delta^{18}O$ increases

$\delta^{18}O_{PC}$ values from other East African sites in-

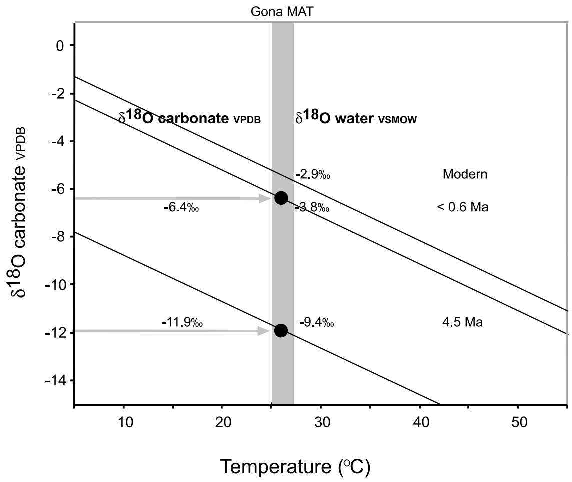

Fig. 7. Lines of constant $\delta^{18}O_{MW}$ values (VSMOW) are plotted with soil temperature and $\delta^{18}O_{PC}$ values (VPDB) according to the temperature-dependent $^{18}O/^{16}O$ calcite–water fractionation, as defined by Kim and O'Neil [44]. The minimum unevaporated $\delta^{18}O_{GW}$ value (−2.9‰) represents the modern mean annual $\delta^{18}O_{MW}$ value (see Fig. 6 and discussion). $\delta^{18}O_{MW}$ values are calculated from minimum 4.5 Ma and < 0.6 Ma $\delta^{18}O_{PC}$ values at 26ˇgC and plotted as lines. The vertical gray bar marks approximate mean annual temperature at Gona today (26ˇgC) and extends to include possible higher mean annual temperatures in the Plio–Pleistocene.

crease through the Plio–Pleistocene and exhibit a large range of values at all time intervals (Fig. 5b) [8–10,40–43,46]. Just as the $\delta^{18}O_{PC}$ values at Gona cannot be reasonably matched with the isotopic composition of modern meteoric waters, $\delta^{18}O_{PC}$ values from elsewhere in Plio–Pleistocene East Africa are also too low to have formed from their local modern waters.

In addition to pedogenic carbonate, gastropods also record the large differences between $\delta^{18}O$ values of Pliocene and modern waters. In their isotopic study of gastropod shells from the Hadar Formation, Hailemichael et al. [12] calculate that $\delta^{18}O_{MW}$ values were 6–7‰ lower at 3.2 Ma than they are today. This estimate is remarkably close to our estimate of a minimum 6.5‰ increase in $\delta^{18}O_{MW}$ values at Gona. The similarity of $\delta^{18}O$ records at Gona and elsewhere in East Africa suggests that the variability of $\delta^{18}O_{PC}$ values and the general increase in $\delta^{18}O_{MW}$ values are regional phenomena that require regional explanations.

6.4. Determinants of $\delta^{18}O_{MW}$ values

Temperature, elevation, precipitation amount and moisture source determine modern $\delta^{18}O_{MW}$ values [27]. One or more of these variables must have changed at a regional scale since the early Pliocene to explain the 6.5‰ increase in $\delta^{18}O_{MW}$ values at Gona and similar changes elsewhere in East Africa. We use isotopic data of modern precipitation from IAEA stations in East Central Africa [47] to understand how these variables may have influenced Plio–Pleistocene $\delta^{18}O_{MW}$ values. Each variable is presented to investigate possible end-member explanations.

At high latitudes, $\delta^{18}O_{MW}$ values increase with temperature, whereas in the low latitude tropics $\delta^{18}O_{MW}$ values and temperature are not well correlated [48]. Among isotope data stations in East Central Africa, there is no consistent relationship between annual or monthly temperatures and $\delta^{18}O_{MW}$ values [47]. We therefore can exclude an increase in temperature as a significant influence on the net 6.5‰ increase in average $\delta^{18}O_{MW}$ values.

The negative correlation seen globally between altitude and $\delta^{18}O_{MW}$ values allows us to test the effect of elevation on the increase of $\delta^{18}O_{MW}$ values at Gona [48]. Several studies have proposed a 1000 m decrease in basin elevation as an explanation for ecological change in the Hadar region [14,49]. Based on the $\delta^{18}O_{MW}$–elevation relationship established for Mt. Cameroon, a 1000 m decrease in elevation would only account for a 1.6‰ increase in $\delta^{18}O_{MW}$ values [50]. Higher basin elevations in the early Pliocene therefore cannot be a primary explanation for the lower $\delta^{18}O_{MW}$ values at Gona.

$\delta^{18}O_{MW}$ values from stations in East Central Africa decrease with increased precipitation, following a trend termed the 'amount effect' [27]. The amount effect, determined from the slope of the linear regression between mean monthly $\delta^{18}O_{MW}$ values and the amount of precipitation, varies with each station. We calculated that the average 'amount effect' for East Central African stations is −32 mm rainfall per 1‰ $\delta^{18}O_{MW}$ [47]. If a change in the amount of precipitation were responsible for the 6.5‰ increase in $\delta^{18}O_{MW}$ values then total annual precipitation would have been approximately 700 mm in the early Pliocene (200 mm more than today). Most IAEA stations in East Central Africa receive more than 700 mm of annual rainfall, yet their minimum monthly $\delta^{18}O_{MW}$ values average −4‰ and are rarely less than −7.3‰ (VSMOW), compared to −9.4‰ (VSMOW) which is the reconstructed mean annual $\delta^{18}O_{MW}$ value for the early Pliocene at Gona. This implies that a decrease in the amount or intensity of precipitation cannot fully explain the increase in $\delta^{18}O_{MW}$ values at Gona through time.

Our analysis suggests that the increase in $\delta^{18}O_{MW}$ values must be partially due to changes in moisture sources or seasonal proportions of moisture sources since the early Pliocene. Moisture sources in East Africa today are governed by the position of major convergence zones, topography and sea-surface temperatures [51,52]. The Intertropical Convergence Zone (ITCZ) separates northeasterly dry Saharan air from easterly and southeasterly air currents sourced in southern Asia and the Indian Ocean. The Interoceanic Convergence (IOC), fixed by the high western shoulders of the East African Rift, separates southwesterly moisture from the Congo and the Atlantic Ocean from southeasterly Indian Ocean moisture. Heavy rains accompany the passage of the ITCZ, yielding only one dominant rainy season in Ethiopia at the ITCZ's northern limit [28]. The aridity in East Africa today is due primarily to high topography that blocks Atlantic moisture, cool upwelling waters near the Somali coast and the subsiding Somali jet which parallels the East African coast [53].

7. Plio–Pleistocene climate change

Any shift in the position of the ITCZ or IOC could alter the source, timing and amount of rainfall in East Africa and consequently alter mean annual $\delta^{18}O_{MW}$ values. Tectonic changes and northern hemispheric glaciation in the Pliocene reorganized East African climate with changes in circulation patterns, increased climate variability and decreased rainfall. We present the following examples of Plio–Pleistocene climate phenomena as possible explanations for the regional changes in mean annual $\delta^{18}O_{MW}$ values, soil water evaporation and the range in environmental conditions evident at Gona and elsewhere in East Africa.

Cane and Molnar [54] suggest that the closure of the Indonesian seaway 3–4 Ma is responsible for increased aridity in East Africa. The authors propose that a northward displacement of New Guinea channeled cool waters from the North Pacific towards the Indian Ocean and blocked the passage of warmer waters from the South Pacific. Periods of heavy rainfall in East Africa today are associated with warm sea-surface temperatures in the Indian Ocean, which reduce air subsidence over East Africa and heat the normally cold upwelling waters along the Somali coast [51]. If the climate behaved similarly in the early Pliocene, a cooling of the Indian Ocean after 3–4 Ma would decrease rainfall in East Africa [54].

The continued development of the high topography of the East African Rift through the Plio–Pleistocene might also contribute to the increase in $\delta^{18}O_{MW}$ values. The East African highlands today block southwesterly Atlantic moisture [53]. Lower topography in the early Pliocene would allow more southwesterly Atlantic moisture to reach East Africa. The associated changes in moisture source and increased rainfall could be partially responsible for lower $\delta^{18}O_{MW}$ values in the early Pliocene.

The closure of the Indonesian seaway is a discrete event, the uplift of the East African highlands is a gradual phenomenon but northern hemispheric glaciation is a cyclic process whose effect repeatedly and drastically altered Plio–Pleistocene climate. Marine dust records and general circulation models for the Plio–Pleistocene show that during full glacial periods and times of reduced summer insolation, increased snow and ice cover in southern Asia inhibits summer heat flow, reduces summer monsoon winds in southwest Asia and reduces precipitation over Africa [4]. Northern hemispheric glaciation also alters the latitudinal position of the ITCZ which depends on the temperature difference between the northern and southern hemispheres. Before the start of northern hemispheric glaciation in the late Miocene, colder temperatures in the southern hemisphere strengthened the southern trade winds and displaced the ITCZ northern limit to 22°N [55]. As the northern hemisphere cooled with the onset of glaciation and as the Central American seaway closed, the ITCZ shifted southward to its present location, 12°N, 4.4–4.3 Ma [55,56]. A more northerly position of the ITCZ in the early Pliocene and during interglacial periods would increase rainfall, alter circulation patterns and lower $\delta^{18}O_{MW}$ values in areas near the present northern limit of the ITCZ. Today, Gona is just south of the ITCZ northern limit.

Glacial and interglacial conditions oscillated on 23/19 kyr, 40 kyr and 100 kyr cycles from the Pliocene through the Pleistocene [57]. East African climate responded to these cycles with changes in moisture source and rainfall amount as described above. Late Pleistocene and early Holocene groundwaters from northern Africa indicate that $\delta^{18}O_{MW}$ values were lower during African wet phases [58–60]. Similarly, speleothem $\delta^{18}O$ values from the Oman indicate that $\delta^{18}O_{MW}$ values increased up to 9.4‰ between interglacial and glacial periods [61]. Fleitmann et al. [61] attribute the difference in $\delta^{18}O_{MW}$ values between interglacial and glacial periods to changes in moisture source with the oscillation of ITCZ position.

An increase in mean annual $\delta^{18}O_{MW}$ values, high variability in environmental conditions, and an increase in soil water evaporation are evident in the Plio–Pleistocene $\delta^{18}O_{PC}$ record at Gona and throughout East Africa. These trends are likely responses to the regional changes in circulation patterns, reduction in rainfall and climatic fluctuations that characterize Plio–Pleistocene climate in East Africa. Given the 100 kyr temporal resolution of the Gona record and the high frequency of climatic events in the Plio–Pleistocene we only explain the $\delta^{18}O_{PC}$ values in terms of general climatic trends. However, with a better understanding of modern $\delta^{18}O_{MW}$ values and the timing of the increase in $\delta^{18}O_{MW}$ values in the Plio–Pleistocene, it might be possible to connect changes in local environmental records to specific regional climate events.

8. Conclusions

Plio–Pleistocene $\delta^{13}C_{PC}$ and $\delta^{18}O_{PC}$ values at Gona and in East Africa indicate a gradual grassland expansion, changing circulation patterns, increased aridity, and strong environmental variability. A combination of global, regional and local climatic factors may be responsible for these trends.

The increase in C_4 grasses at Gona through the Plio–Pleistocene reflects both a local shift in depositional environment and the East African expansion of C_4 grasslands in the late Neogene [6]. Increasing aridity or a change in the seasonal distribution of rainfall, as indicated by the increase in $\delta^{18}O_{PC}$ values, are possible explanations for this vegetation shift at Gona. However, a greater abundance of C_4 plants is also evident at Gona across a major facies shift at $\sim$1.5 Ma between the lower Busidima Formation, where water is available on the landscape in lakes or active floodplains, and the upper Busidima Formation, where small tributary rivers host water-stressed environments. The Gona record demonstrates that changes in C_3/C_4 vegetation must be examined within their depositional context before assigning regional significance to any changes.

$\delta^{18}O_{PC}$ values from Gona and other East African sites point to an increase in $\delta^{18}O_{MW}$ values, greater aridity and high climate variability through the Plio–Pleistocene. The comparison between early Pliocene $\delta^{18}O_{PC}$ values and modern $\delta^{18}O_{MW}$ values demonstrates that $\delta^{18}O_{MW}$ values have increased by at least 6.5‰ since 4.5 Ma. We attribute low $\delta^{18}O_{MW}$ values in the Pliocene to a regional change in moisture source. Smaller-scale climate fluctuations that influence $\delta^{18}O_{MW}$ values and evaporative conditions are responsible for the large range of $\delta^{18}O_{PC}$ values at all stratigraphic levels.

The expansion of grasslands, changing $\delta^{18}O_{MW}$ values and increased aridity are probable responses to the onset of glaciation and the reorganization of atmospheric circulation in East Africa during the Plio–Pleistocene. However, the terrestrial expression of global or regional climate phenomena depends on local conditions. As we better characterize specific paleoenvironments and their response to regional climatic trends, paleoenvironmental studies will become increasingly meaningful to questions concerning human evolution.

Acknowledgements

We thank K. Schick and N. Toth of CRAFT at Indiana University, the ARCCH of the Ministry of Youth, Sports and Culture of Ethiopia, the National Museum of Addis Ababa, and the Afar people of Elowaha who made this project possible. D. Dettman and A. Cohen provided useful comments on the manuscript. We appreciate the instructive reviews of D. Deocampo and P. Koch. This research was funded by grants to S.S. from the Leakey Foundation, the Wenner-Gren Foundation, the National Geographic Society and the National Science Foundation (Grant SBR-9910794).***[BOYLE]***

References

[1] S.W. Simpson, S. Semaw, K. Schick, N. Toth, J. Quade, M. Dominguez-Rodrigo, M.J. Rogers, Early Pliocene hominid remains from Gona, Ethiopia, J. Hum. Evol. 40 (2001) A21–A22.

[2] S. Semaw, K. Schick, N. Toth, M.J. Rogers, J. Quade, S.W. Simpson, M. Dominguez-Rodrigo, Further 2.5–2.6 million year old artifacts, new Plio-Pleistocene archaeological sites and hominid discoveries of 1999 from Gona Ethiopia, J. Hum. Evol. 40 (2001) A20.

[3] S. Semaw, P. Renne, J.W.K. Harris, C.S. Feibel, R.L. Bernor, N. Fesseha, K. Mowbray, 2.5-million-year-old stone tools from Gona, Ethiopia, Nature 385 (1997) 333–336.

[4] P.B. deMenocal, J. Bloemendal, Plio-Pleistocene climatic variability in subtropical Africa and the paleoenvironment of hominid evolution: a combined data-model approach, in: E.S. Vrba, G.H. Denton, T.C. Partridge, L.H. Burckle (Eds.), Paleoclimate and Evolution with an Emphasis on Human Origins, Yale University Press, New Haven, CT, 1995, pp. 262–288.

[5] J.R. Marlow, C.B. Lange, G. Wefer, A. Rosell-Mele, Upwelling intensification as part of the Pliocene-Pleistocene climate transition, Science 290 (2000) 2288–2291.

[6] T.E. Cerling, J.M. Harris, B.J. MacFadden, M.G. Leakey, J. Quade, V. Eisenmann, J.R. Ehleringer, Global vegetation change through the Miocene/Pliocene boundary, Nature 389 (1997) 153–158.

[7] A.K. Behrensmeyer, N.E. Todd, R. Potts, G.E. McBrinn, Late Pliocene faunal turnover in the Turkana Basin, Kenya and Ethiopia, Science 278 (1997) 1589–1594.

[8] T.E. Cerling, J.R. Bowman, J.R. O'Neil, An isotopic study of a fluvial-lacustrine sequence: the Plio-Pleistocene Koobi Fora sequence, East Africa, Palaeogeogr. Palaeoclimatol. Palaeoecol. 63 (1988) 335–356.

[9] T.E. Cerling, R.L. Hay, An isotopic study of paleosol carbonates from Olduvai Gorge, Quat. Res. 25 (1986) 63–78.

[10] G. Wolde Gabriel, Y. Haile-Selassie, P.R. Renne, W.K. Hart, S.H. Ambrose, B. Asfaw, G. Heiken, T. White, Geology and paleontology of the Late Miocene Middle Awash valley, Afar rift, Ethiopia, Nature 412 (2001) 175–178.

[11] C. Hillaire-Marcel, M. Taieb, J.J. Tiercelin, N. Page, A 1.2-Myr record of isotopic changes in a late Pliocene Rift Lake, Ethiopia, Nature 296 (1982) 640–642.

[12] M. Hailemichael, J.L. Aronson, S. Savin, M.J.S. Tevesz, J.G. Carter, $\delta^{18}O$ in mollusk shells from Pliocene Lake Hadar and modern Ethiopian lakes: implications for history of the Ethiopian monsoon, Palaeogeogr. Palaeoclimatol. Palaeoecol. 186 (2002) 81–99.

[13] T. Gray, Environmental Reconstruction of the Hadar Formation (Afar, Ethiopia), Ph.D. Dissertation, Case Western Reserve University, Cleveland, OH, 1980.

[14] R. Bonnefille, A. Vincens, G. Buchet, Palynology, Stratigraphy and Palaeoenvironment of a Pliocene hominid site (2.9–3.3 M.Y.) at Hadar, Ethiopia, Palaeogeogr. Palaeoclimatol. Palaeoecol. 60 (1987) 249–281.

[15] J.J. Tiercelin, The Pliocene Hadar Formation, Afar depression of Ethiopia, in: L.E. Frostick, R.W. Renaut, I. Reid, J.J. Tiercelin (Eds.), Sedimentation in the African Rifts, Blackwell Scientific, Oxford, 1986, pp. 221–240.

[16] J. Quade, N. Levin, S. Semaw, D. Stout, P. Renne, M. Rogers, S.W. Simpson, Paleoenvironments of the earliest stone toolmakers, Gona, Ethiopia, Geol. Soc. Am. Bull. (submitted).

[17] R.C. Walter, Age of Lucy and the first family; single-crystal $^{40}Ar/^{39}Ar$ dating of the Denen Dora and lower Kada Hadar members of the Hadar Formation, Ethiopia, Geology 22 (1994) 6–10.

[18] T.E. Cerling, J.M. Harris, B.H. Passey, Diets of East African bovidae based on stable isotopic analysis, J. Mammal. 84 (2003) 456–470.

[19] L.L. Tieszen, M.M. Senyimba, S.K. Imbamba, J.H. Troughton, The distribution of C_3 and C_4 grasses and carbon isotope discrimination along an altitudinal and moisture gradient in Kenya, Oecologia 37 (1979) 337–350.

[20] D.A. Livingstone, W.D. Clayton, An altitudinal cline in tropical African grass floras and its paleoecological significance, Quat. Res. 13 (1980) 392–402.

[21] T.E. Cerling, The stable isotopic composition of modern soil carbonate and its relationship to climate, Earth Planet. Sci. Lett. 71 (1984) 229–240.

[22] T.E. Cerling, J. Quade, Stable carbon and oxygen isotopes in soil carbonates, AGU Geophys. Monogr. 78 (1993) 217–231.

[23] J. Lee Thorp, N.J. van der Merwe, Carbon isotope analysis of fossil bone apatite, S. Afr. J. Sci. 83 (1987) 712–715.
[24] T.E. Cerling, J.M. Harris, Carbon isotopic fractionation between diet and bioapatite in ungulate mammals and implications for ecological and paleoecological studies, Oecologia 120 (1999) 347–363.
[25] C.D. Keeling, R.B. Bacastow, A.F. Carter, S.C. Piper, T.P. Whorf, M. Heimann, W.G. Mook, H. Roeloffzen, A three-dimensional model of atmospheric CO_2 transport based on observed winds: 1. Analysis of observational data, in: D.H. Peterson (Ed.), Aspects of Climate Variability in the Pacific and the Western Americas, American Geophysical Union, Washington, DC, 1989, pp. 165–236.
[26] B.H. Passey, T.E. Cerling, M. Perkins, E.M.R. Voorhies, J.M. Harris, S.T. Tucker, Environmental change in the Great Plains: an isotopic record from fossil horses, J. Geol. 110 (2002) 123–140.
[27] W. Dansgaard, Stable isotopes in precipitation, Tellus 16 (1964) 436–468.
[28] K. Rozanski, L. Araguas-Araguas, R. Gonfiantini, Isotope patterns of precipitation in the East African region, in: T.C. Johnson, E.O. Odada (Eds.), The Limnology, Climatology and Paleoclimatology of the East African Lakes, Gordon and Breach, London, 1996, pp. 79–93.
[29] J. Quade, T.E. Cerling, J.R. Bowman, Systematic variations in the carbon and oxygen isotopic composition of pedogenic carbonate along elevation transects in the southern Great Basin, United States, Geol. Soc. Am. Bull. 101 (1989) 464–475.
[30] D. Hillel, Introduction to Soil Physics, Academic Press, London, 1982, 364 pp.
[31] J.R. O'Neil, L.J. Roe, E. Reinhard, R.E. Blake, A rapid and precise method of oxygen isotope analyses of biogenic phosphate, Isr. J. Earth Sci. 43 (1994) 203–212.
[32] S. Epstein, T. Mayeda, Variations in ^{18}O content of waters from natural sources, Geochim. Cosmochim. Acta 4 (1953) 213–224.
[33] M. Gehre, R. Hoefling, P. Kowski, G. Strauch, Sample preparation device for quantitative hydrogen isotope analysis using chromium metal, Anal. Chem. 68 (1996) 4414–4417.
[34] L.H. Gile, F.F. Peterson, R.B. Grossman, Morphological and genetic sequences of carbonate accumulation in desert soils, Soil Sci. 101 (1966) 347–360.
[35] H. Bao, P.L. Koch, R.P. Hepple, Hematite and calcite coatings on fossil vertebrates, J. Sediment. Res. 68 (1998) 727–738.
[36] H.C. Monger, L.A. Daugherty, L.H. Gile, A microscopic examination of pedogenic calcite in an aridisol of southern New Mexico, in: W.D. Nettleton (Ed.), Occurrence, Characteristics, and Genesis of Carbonate, Gypsum, and Silica Accumulations in Soils, Soil Science Society of America, Madison, WI, 1991.
[37] Y. Wang, T.E. Cerling, A model of fossil tooth and bone diagenesis: Implications for paleodiet reconstruction from stable isotopes, Palaeogeogr. Palaeoclimatol. Palaeoecol. 107 (1994) 281–289.
[38] J.R. Ehleringer, N. Buchmann, L.B. Flanagan, Carbon isotope ratios in belowground carbon cycle processes, Ecol. App. 10 (2000) 412–422.
[39] M.E. Morgan, J.D. Kingston, B.D. Marino, Carbon isotopic evidence for the emergence of C4 plants in the Neogene from Pakistan and Kenya, Nature 367 (1994) 162–165.
[40] N.E. Sikes, Early hominid habitat preferences in East Africa: Paleosol carbon isotopic evidence, J. Hum. Evol. 27 (1994) 25–45.
[41] N.E. Sikes, R. Potts, A.K. Behrensmeyer, Early Pleistocene habitat in Member 1 Olorgesailie based on paleosol stable isotopes, J. Hum. Evol. 37 (1999) 721–746.
[42] J.G. Wynn, Paleosols, stable carbon isotopes, and paleoenvironmental interpretation of Kanapoi, Northern Kenya, J. Hum. Evol. 39 (2000) 411–432.
[43] T. Plummer, L.C. Bishop, P. Ditchfield, J. Hicks, Research on Late Pliocene Oldowan sites at Kanjera South, Kenya, J. Hum. Evol. 36 (1999) 151–170.
[44] S.-T. Kim, J.R. O'Neil, Equilibrium and nonequilibrium oxygen isotope effects in synthetic carbonates, Geochim. Cosmochim. Acta 61 (1997) 3461–3475.
[45] R. Gonfiantini, Environmental isotopes in lake studies, in: P. Fritz, J.C. Fontes (Eds.), Handbook of Environmental Isotope Geochemistry, Elsevier, Amsterdam, 1986, pp. 113–168.
[46] J.D. Kingston, Stable Isotopic Evidence for Hominid Paleoenvironments in East Africa, Ph.D. Dissertation, Harvard University, Cambridge, MA, 1992.
[47] IAEA, Isotope Hydrology Information System, http://isohis.iaea.org, 2001.
[48] K. Rozanski, L. Araguas-Araguas, R. Gonfiantini, Isotopic patterns in modern global precipitation, AGU Geophys. Monogr. 78 (1993) 1–36.
[49] C. Denys, J. Chorowicz, J.J. Tiercelin, Tectonic and environmental control on rodent diversity in the Plio-Pleistocene sediments of the African Rift system, in: L.E. Frostick, R.W. Renaut, I. Reid, J.J. Tiercelin (Eds.), Sedimentation in the African Rifts, Blackwell Scientific, Oxford, 1986, pp. 363–372.
[50] R. Gonfiantini, M.-A. Roche, J.-C. Olivry, J.-C. Fontes, G.M. Zuppi, The altitude effect on the isotopic composition of tropical rains, Chem. Geol. 181 (2001) 147–167.
[51] L. Goddard, N.E. Graham, Importance of the Indian Ocean for simulating rainfall anomalies over eastern and southern Africa, J. Geophys. Res. 104 (1999) 19099–19116.
[52] S.E. Nicholson, A review of climate dynamics and climate variability in Eastern Africa, in: T.C. Johnson, E.O. Odada (Eds.), The Limnology, Climatology and Paleoclimatology of the East African Lakes, Gordon and Breach, London, 1996, pp. 25–56.
[53] H. Flohn, Studies on the meteorology of tropical Africa, Bonner Meteorol. Abh. 5 (1965) 57 pp.
[54] M.A. Cane, P. Molnar, Closing of the Indonesian seaway

as a precursor to east African aridification around 3–4 million years ago, Nature 411 (2001) 157–162.

[55] D.K. Rea, The paleoclimatic record provided by eolian deposition in the deep sea: the geologic history of wind, Rev. Geophys. 32 (1994) 159–195.

[56] K. Billups, A.C. Ravelo, J.C. Zachos, R.D. Norris, Link between oceanic heat transport, thermohaline circulation, and the Intertropical Convergence Zone in the early Pliocene Atlantic, Geology 27 (1999) 319–322.

[57] J. Imbrie, E.A. Boyle, S.C. Clemens, A. Duffy, W.R. Howard, G. Kukla, J. Kutzbach, D.G. Martinson, A. McIntyre, A.C. Mix, B. Molfino, J.J. Morley, L.C. Peterson, N.G. Pesias, W.L. Prell, M.E. Raymo, N.J. Shackleton, J.R. Toggweiler, On the structure and origin of major glaciation cycles, Pt. 1. Linear responses to Milankovitch forcing, Paleoceanography 7 (1992) 701–738.

[58] U. Beyerle, J. Rueedi, M. Leuenberger, W. Aesch-Hertig, F. Peeters, R. Kipfer, A. Dodo, Evidence for periods of wetter and cooler climate in the Sahel between 6 and 40 kyr BP derived from groundwater, Geophys. Res. Lett. 30 (2003) 1173.

[59] M. Sultan, N. Sturchio, F.A. Hassan, M.A.R. Hamdam, A.M. Mahmood, Z. El Alfy, T. Stein, Precipitation source inferred from stable isotopic composition of Pleistocene groundwater and carbonate deposits in the western desert of Egypt, Quat. Res. 48 (1997) 29–37.

[60] J.-C. Fontes, F. Gasse, J.N. Andrews, Climatic conditions of Holocene groundwater recharge in the Sahel zone of Africa, in: Isotopic Techniques in the Study of Past and Current Environmental Changes in the Hydrosphere and the Atmosphere, Vienna, 1993, pp. 231–248.

[61] D. Fleitmann, S.J. Burns, U. Neff, A. Mangini, Changing moisture sources over the last 330,000 years in Northern Oman from fluid-inclusion evidence in speleothems, Quat. Res. 60 (2003) 223–232.